A Nanomanipulation System Based on A Sample-Scanning AFM

Xiaojun Tian Lianqing Liu Niandong Jiao Ning Xi Yuechao Wang Zaili Dong

Abstract—**Atomic Force Microscope (AFM) has been proven to be a useful tool to characterize and change the sample surface down to the nanometer scale. However, in the AFM based nano manipulation, the main problem is the lack of real-time sensory feedback for an operator, which makes the manipulation almost in the dark and inefficient. For solving this problem, the AFM probe micro cantilever-tip is used not only as an end effector but also as a 3D nano forces sensor for sensing the interactive forces between the AFM probe tip and the object or substrate in nanomanipulation, and a kind of new and relatively easier parameters obtainment or calibration method in forces calculation has also been presented. In addition, for further improving probe positioning accuracy with a sample-scanning AFM, two important errors in probe positioning are quantitatively analyzed according to the tube scanner kinematics model presented in this paper, corresponding methods are adopted for minimizing the two errors and thus the probe positioning accuracy can be greatly improved. With 3D nano forces sensing through a haptic/force device and probe positioning accuracy improvement, the efficiency and accuracy of nano manipulation can be significantly improved. Experiments are presented to verify the effectiveness of the nanomanipulation system.**

Index Terms—**AFM, Nanomanipulation, 3D Nano Forces Sensing, Probe Positioning Errors Minimizing**

Ⅰ. INTRODUCTION

Atomic Force Microscope [1] (AFM) has been proven to be a useful tool to study sample surfaces down to the nanometer scale. More importantly, not only can it image sample surfaces, it can also change the sample surface through various kinds of manipulation. The AFM has provided a tool to manipulate materials and structure in the nanometer scale, and recently several kinds of manipulation methods have been presented [2], [3], [4], [5]. However, in these AFM based nano manipulation, the main problem is the lack of real-time sensory feedback for an operator, and the manipulation is almost conducted in the dark. The results can only be verified by another new scanning image for every manipulation step, and apparently these kinds of nanomanipulation are inefficient.

Manuscript received May 14, 2004. This research work was partially supported by NHTRDP (863 program) Grants 2002AA422210 and 2003AA404070.

Xiaojun Tian, Lianqing Liu, Niandong Jiao, Yuechao Wang and Zaili Dong are with Shenyang Institute of Automation, CAS, China. And Xiaojun Tian, Niandong Jiao, Lianqing Liu are also with Graduate School, CAS, China. (Tel: 024-23970540, Fax: 024-23970021, Email: xjtian@sia.cn)

Ning Xi is with the Department of Electrical and Computer Enginerring, Michigan State University, U.S.A.

In recent years, several researchers have tried to integrate AFM with haptic technique to assist nanomanipulation [6], [7], in which a 1 degree of freedom (DOF) haptic device had been constructed for feeling the vertical force acting on AFM probe tip. However, in one hand, haptic/force feedback technique used by them is very difficult to be implemented due to many unmeasurable forces and parameters in the nano-situation such as Van der Walls force and capillary force, etc. In another hand, horizontal forces acting on tip are ignored, which results in the information shortage for comprehensively feeling nanomanipulation situation and guiding manipulation.

In this paper, the AFM probe cantilever deflection-force model is presented for obtaining the 3D forces in nano situation according to real-time PSD signals which reflect the cantilever deflections during nano manipulation. In 3D nano forces calculation formula, there are several parameters needed to be calibrated, and for in practice it is very difficult and time-consuming to get or calibrate the force parameters according to methods proposed by some researchers [8], [9] etc, a kind of new and relatively easier parameters obtainment or calibration method is also presented in force calculation.

Additionally, previous nanomanipulations are almost implemented by a tip-scanning AFM, where the bow effect only causes the vertical cross-coupling error of probe positioning which can be ignored for small manipulating area. However, for a sample-scanning AFM, two important errors in probe positioning will be generated, namely scanning size error and cross coupling error, which are caused by bend motion of tube scanner, and these two errors are destructive to nano manipulation accuracy. To minimize the two errors, in this paper a kinematics model of the scanner is presented, the two errors are quantitatively analyzed according to the model and corresponding methods are proposed for minimizing them.

After the real-time 3D nano forces are obtained using the method presented in this paper, they are augmented and sent to a haptic device for user to feel. Furthermore, the operator can directly control the motion of the scanner which drives the sample to move relative to the probe tip through the haptic device's joystick. And with the two errors minimizing, the probe tip positioning accuracy can be greatly improved. As a result, the operator can accurately conduct nanomanipulation in nanoenvironment under the assistance of real-time haptic/force feedback, and the efficiency and accuracy of nano manipulation can be significantly improved. The experimental testing results are presented to demonstrate effectiveness of this nanomanipulation system.

Ⅱ. 3D NANO FORCES SENSING

A 3D Nano Forces Applied on Cantilever-Tip

During nanomanipulation, the probe tip will be subject to various kinds of nano forces such as Van del Walls force, capillary force, electrostatic force, contact repulsive force, frictional force et al. [10], and all these forces applied on tip will make cantilever deflect with bend and twisting. The resultant force applied on tip can be simplified as 3D forces, namely F_x, F_y and F_z, along three coordinate axes as shown in Fig. 1.

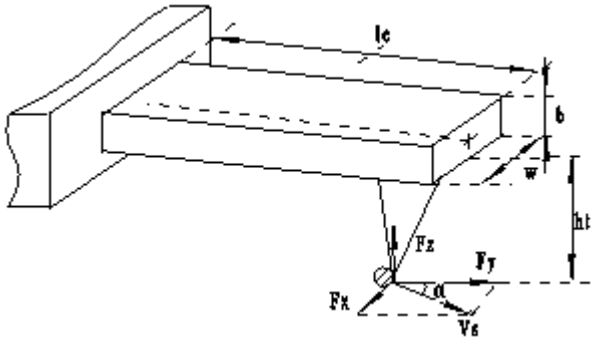

Fig. 1. Model of cantilever-tip subject to 3D nano forces

Since the nano manipulation task is implemented by the very front part of tip which is very small compared with the whole probe tip body, the forces applied on tip can be viewed as applied on tip apex.

In the three forces, the force F_x will twist the cantilever around its center axis with the twisting angle (θ_x), and it can be obtained by

$$F_x(h_t + b/2) = k_{ct}\theta_x \tag{1}$$

Where, h_t is the height of tip, b is thickness of cantilever, k_{ct} is the torsion strength of cantilever.

The forces F_z and F_y will make the cantilever bend in vertical plane, and the vertical deflection of the cantilever (δ_z) can be presented as

$$F_z l_c + F_y(h_t + b/2) = k\delta_z l_c \tag{2}$$

Where, l_c is the length of cantilever, k is the force constant of cantilever.

Assume the sample moves relative to cantilever center axis with angle (α), the relationship between forces F_y and F_x will be

$$F_y = F_x c\tan\alpha \tag{3}$$

With forces applied on tip, the cantilever deflections will happen. The cantilever deflections are detected optically by collecting reflected laser off the cantilever using Position Sensitive Detector (PSD), and the PSD will output signals with vertical signal reflecting the cantilever vertical deflection and horizontal signal reflecting the cantilever twisting deflection. Then δ_z and θ_x can be obtained as

$$\delta_z = k_v S_v \tag{4}$$

$$\theta_x = k_h S_h \tag{5}$$

Where k_v and k_h are system constants, S_v is vertical signal output and S_h is horizontal signal output of PSD which can be presented as

$$S_v = \frac{(S_1 + S_2) - (S_3 + S_4)}{(S_1 + S_2 + S_3 + S_4)}$$

$$S_h = \frac{(S_1 + S_4) - (S_2 + S_3)}{(S_1 + S_2 + S_3 + S_4)}$$

Where, $S_1 \sim S_4$ are voltage signals output of the quad photodiodes as shown in Fig. 2.

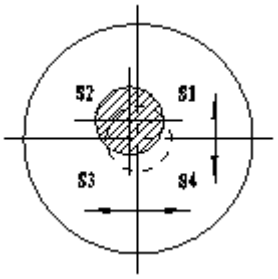

Fig. 2. The quad photodiode detector PSD: $S_1 \sim S_4$ are the signal outputs of the quad photodiodes

With nano forces acting on cantilever-tip analyzed and cantilever deflections obtained by PSD signals, the 3D nano forces can be obtained. Submitting equations (4) and (5) into equations (1)~(3), the 3D forces calculation formulas can be presented as

$$\begin{cases} F_x = k_{ct}k_h S_h/(h_t + b/2) \\ F_y = F_x c\tan\alpha \\ F_z = kk_v S_v - F_y(h_t + b/2)/l_c \end{cases} \tag{6}$$

It can be seen from equation (6) that the real 3D forces can be calculated if the parameters (k_{ct}, k_v, k_h and k) can be obtained and calibrated.

B Parameters Obtainment and Calibration

In order to obtain the real forces acting on the tip by measuring the deflection signals from the quad-photodiodes array, the system constants in above equation (6), such as k_{ct}, k_v, k_h and k, must be obtained and calibrated.

1) k_v

Using Z-axis calibration gratings (MickoMasch Inc., USA) comprising an one-dimensional array of rectangular steps with a calibrated height, move the probe horizontally from the above to the bottom of steps with vertical force feedback off, the cantilever deflection will be the height of step, record the PSD vertical signal with an oscillograph (Tektronix TDS3012B, USA) as shown in Fig.3.

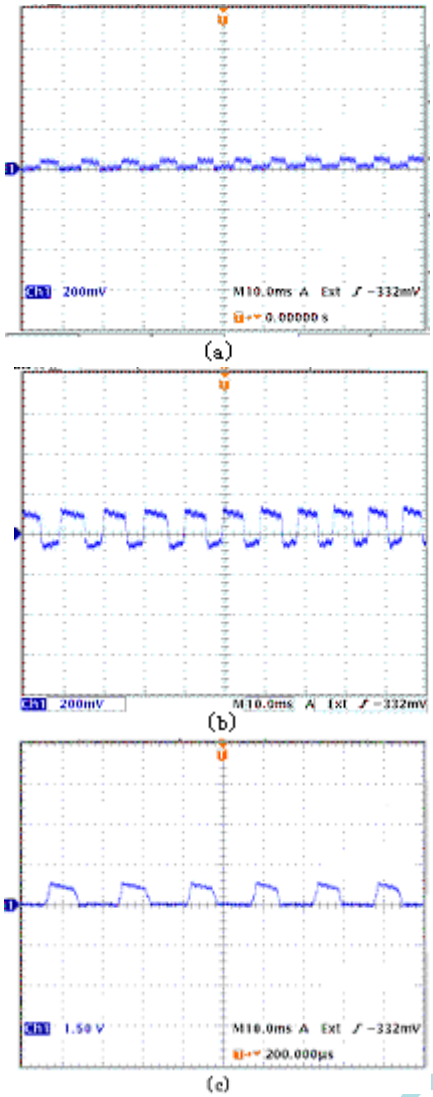

Fig. 3. PSD vertical signal when tip moves on the steps of gratings with different height step while vertical force feedback is off: (a) step height is 20nm; (b) step height is 101.8nm; (c) step height is 500nm

It is shown in Fig. 3. that PSD vertical signal change is 32mv when step height is 20nm, while it is 156mv when step height is 101.8nm, and 710mv to step height 500nm, then the relationship curve of cantilever vertical deflection δz and PSD vertical signal S_v can be obtained as shown in Fig. 4.

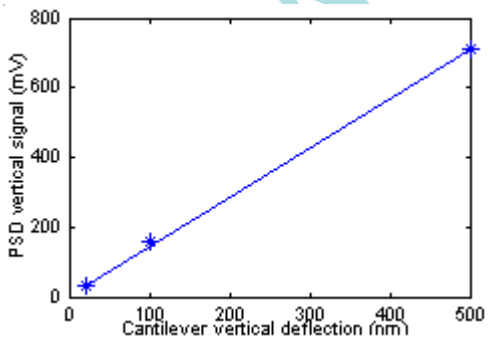

Fig. 4. The relationship curve of the cantilever vertical deflection and PSD vertical signal

Noting that $k_v = \delta_z / S_v$, the parameter k_v can be got from the slope of the line as shown in Fig. 4., that is k_v=706nm/V.

2) k_h

For the quad-photodiode detector has the same sensitivity both in the vertical and the horizontal directions in design, that is, the vertical and horizontal signal outputs should be equal if the vertical bending angle equals to the twisting angle. Usually the two angles are very small, there is $\theta \approx \tan\theta$. So, the vertical bending angle can be viewed as

$$\theta_z \approx \delta_z / l_c = \frac{k_v}{l_c} S_v .$$

Noting that $\theta_x = k_h S_h$ and the same sensitivity both in vertical and horizontal directions, it can be obtained that $k_h = k_v / l_c$, and here we get k_h=0.00565rad/V.

3) k_{ct}

The torsion strength of thin-wall rectangle cantilever can be presented [11] as

$$k_{ct} = G\beta w b^3 / l_c$$

Where G is the shearing elasticity modulus of cantilever materials which is silicon (100), w is the width of cantilever, β is a constant dependent on b/w [9]. Here k_{ct}=8.56*10^{-7}N.m/rad can be got.

4) k

For the exact force constant k of cantilever is very difficult to get in practice, force constant calibrated probe with k =38.6N/m is used here.

III PROBE POSITIONING ERRORS MINIMIZING

For a sample-scanning AFM, two important errors in probe positioning will be generated, namely scanning size error and vertical cross coupling error, and these two errors are destructive to nanomanipulation accuracy. To minimize the two errors, the kinematics model of the scanner is presented, the two errors are quantitatively analyzed according to the model and corresponding methods are presented for minimizing them.

A Kinematics Model of Tube Scanner

Single tube scanner is generally used in AFM [12], common structure of single tube scanner in sample-scanning AFM is shown in Fig. 5.

Fig. 5. Tube scanner structure in sample-scanning AFM

The main part of tube scanner is a piezoceramics tube with one end attached to sample stage, which is free end, and the other end fixed on a base. The inside wall and outside wall of

the tube are plated with metal, and the outside wall is quartered with two opposite electrodes used as one part. When voltage is applied to the inside wall, the vertical displacement of sample will be realized.

When ambipolar voltage is applied on the two opposite electrodes of the outside wall, the tube will bend, and actually sample will generate not only horizontal translation but also rotation in vertical plane as shown in Fig. 6.

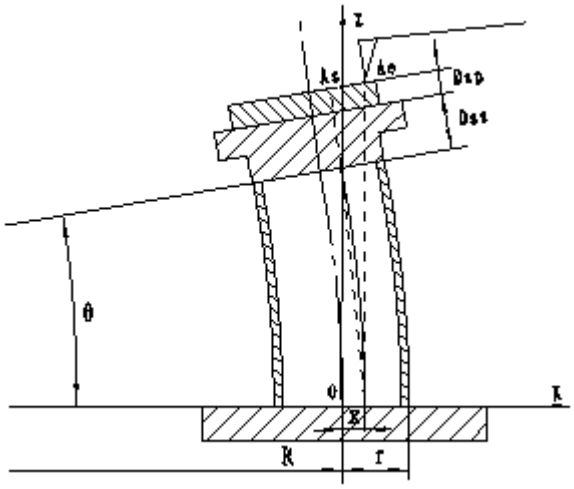

Fig. 6. Kinematics model of single tube scanner of sample-scanning AFM

In Fig. 6., the part clipped by angle θ is piezoceramics tube, the part pointed by Dss is sample stage, and Dsp is sample.

Supposing material of scanner is uniform and structure is symmetric, and scanner axis is viewed as symmetric axis, the extension and condensation will be the same with ambipolar voltage applied to two opposite electrodes, and the bend geometry can be viewed as circular arc [13], then we have

$$\begin{cases}(R+r)\theta=L+\Delta L\\(R-r)\theta=L-\Delta L\end{cases} \tag{7}$$

Where r is the outside radius of tube, R is the curvature radius of the tube axis, θ is the central angle, L is the initial length of tube, and ΔL is the extension of tube after voltage U_x is applied to the tube.

The extension of tube can be presented [14] as

$$\Delta L = Ed_{31}L = \frac{d_{31}L}{t}U_x \tag{8}$$

Where E is the electric field intensity, U_x is voltage along x axis, t is thickness of tube wall, and d_{31} is piezoelectric constant along tube axis.

Submitting equation (8) into (7), one can obtain the expression of θ

$$\theta = \frac{L}{R} = \frac{d_{31}L}{tr}U_x \tag{9}$$

Before tube bends, the horizontal coordinate of the point on sample, corresponding to the probe tip offset to tube axis, is x and vertical coordinate of it is $L + Dss + Dsp$. After tube bends to left as shown in Fig. 6., the point moves to point As, then the displacement of the scanner (or the point on sample) can be presented as

$$dx = (R+x)(1-\cos\theta)+(Dss+Dsp)\sin\theta \tag{10}$$

$$dz = ((R+x)\sin\theta - L)+(Dss+Dsp)(\cos\theta-1) \tag{11}$$

For t, r, L and d_{31} are all constants for a given scanner, then θ or R only depends on U_x according to equation (9), and Dss is also a constant, the lateral and vertical displacements (dx and dz) at any point on sample depend on applied voltage (U_x), its offset to tube axis (x) and sample thickness (Dsp).

B Scanning Size Error, Vertical Cross Coupling Error and Corresponding Minimizing Methods

1) Analysis of Scanning Size and Vertical Coordinate of the Point on Sample Touched by the Probe Tip

As shown in Fig. 6., the horizontal position of the point on sample contacted by probe tip, which is also the center of scanning area, is decided by its offset to scanner axis. And the offset can be adjusted manually by adjusting tube scanner base position before imaging starts.

After tube bending, the sample's point touched by probe tip has changed from point As to point Ae as shown in Fig. 6., and point Ae's vertical coordinate z_{Ae} is

$$Z_{Ae} = (R+x)\tan\theta + (Dss+Dsp)/\cos\theta \tag{12}$$

Thus the right scanning area covers the area from point Ae to point As, and its size can be obtained as

$$Lrss=[(R+x)(1-\cos\theta)+(Dss+Dsp)\sin\theta]/\cos\theta \tag{13}$$

Likewise, when tube bends right, the size of left scanning area $Llss$ can also be obtained as

$$Llss=[(R-x)(1-\cos\theta)+(Dss+Dsp)\sin\theta]/\cos\theta \tag{14}$$

Then the whole actual scanning size (Lss) can be deduced from equations (13) and (14)

$$Lss=2[R(1-\cos\theta)+(Dss+Dsp)\sin\theta]/\cos\theta \tag{15}$$

For Dss is a constant and θ or R only depend on U_x, the scanning size depends on U_x and Dsp.

AFM system needs calibration before operating, and the thickness of the grating used in lateral calibration can be called nominal sample thickness ($Dnsp$). After calibration, scanning size can be called nominal scanning size ($Lnss$), which can be easily changed on user interface, and it can be obtained from equation (15) as

$$Lnss=2[R(1-\cos\theta)+(Dss+Dnsp)\sin\theta]/\cos\theta \tag{16}$$

For $Dnsp$, Dss are constants, $Lnss$ corresponds to θ or R.

2) Scanning Size Error and Minimizing Method

When sample thickness is not equal to nominal one, there will be an error between actual scanning size and nominal

one. From equations (15) and (16), scanning size error ($dLss$) between actual scanning size (Lss) and nominal scanning size ($Lnss$) can be presented as

$$dLss = 2(Dsp - Dnsp)\tan(\theta) \quad (17)$$

For $Dnsp$ is a constant, scanning size error ($dLss$) depends on sample thickness (Dsp) and central angle which corresponds to nominal scanning size ($Lnss$). The calibration grating imaging experiment shows the actual scanning size changes to different sample thickness as shown in Fig. 7.

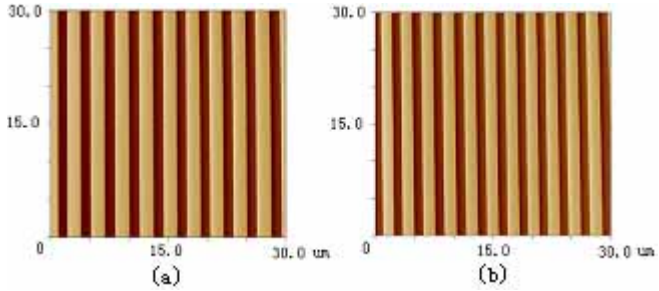

Fig. 7. Two scanning images of grating with different thickness when nominal scanning size is 30um: the grating thickness is 2mm in image (a), the grating thickness is 10mm in image (b). (Step width is 3um in the two images)

It can be seen from Fig.7 that the actual scanning size will increase with sample thickness increasing. For minimizing the scanning size error in nanomanipulation, the sample thickness is increased or decreased to make it equal to nominal one in practice.

3) Vertical Cross Coupling Error and Minimizing Method

Before tube bending, the initial vertical coordinate of the point on sample touched by probe tip is $L + Dss + Dsp$. While after tube bending, the vertical coordinate of the point on sample touched by probe tip is shown in equation (12), thus the vertical cross coupling error (dZr) can be presented as

$$dZr = [(R+x)\tan\theta - L] + [(Dss + Dsp)(1/\cos\theta - 1)] \quad (18)$$

For Dss , L are constants and θ or R corresponds to nominal scanning size, the vertical cross coupling error (dZr) depends on probe tip offset to tube axis (x), nominal scanning size ($Lnss$) and sample thickness (Dsp) as shown in Fig. 8.

It can be seen that the step is slant in image (b) of Fig. 8. although it is horizontal when it keeps still, and the slant will increase with tip offset increasing, which means the vertical cross coupling increases with tip offset increasing. For minimizing vertical cross coupling error in nanomanipulation, tip offset to tube axis is firstly adjusted to zero by manually adjusting the horizontal position of tube scanner base until the sample section image becomes horizontally "bow"-shaped in practice.

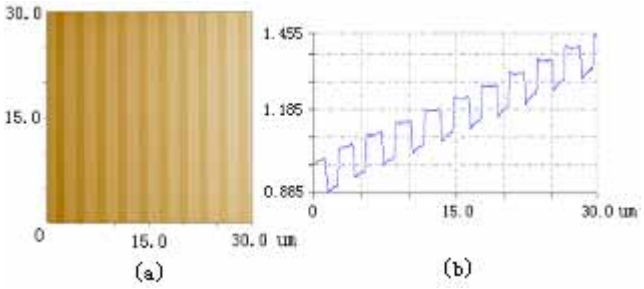

Fig. 8. Scanning image (a) and its cross section image (b) of grating with tip offset equal to 0.5mm when scanning size is 30um (the effect of hysteresis and creep on imaging can be also observed in image (b))

Ⅳ EXPERIMENTS VERIFICATION

In order to verify the effectiveness of the nanomanipulation system, nano-imprint is performed and the 3D nano forces are recorded real-time during nano-imprinting.

A System Configuration

A sample-scanning AFM (model CSPM-2000wet, Ben Yuan Ltd., China) was used for imaging and nanomanipulation. A scanner is equipped in the AFM head with a maximum XY scan range of 50um X 50um and a Z range of 5um.The AFM based nano manipulation system is shown in Fig. 9.

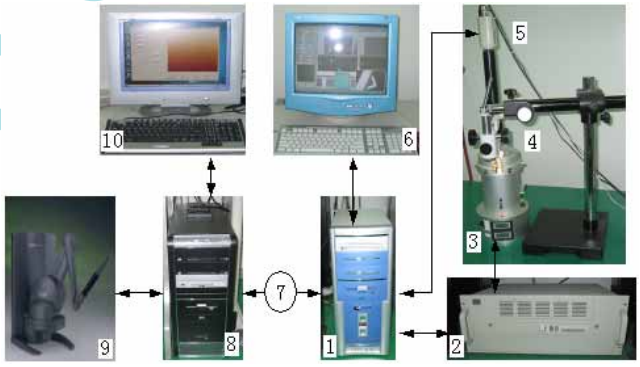

Fig. 9. The configuration of AFM based nanomanipulation system: 1, AFM control computer; 2, CSPM 2000wet controller; 3, AFM head; 4, optical microscope; 5, CCD camera; 6, Monitor for imaging show and optical vision; 7, Ethernet device; 8, Second computer; 9, Haptic device; 10, monitor for haptic manipulation interface

In the system, the cantilever deflection signals obtained by PSD, mounted in AFM head, go into the A/D convertor card inside the AFM control computer and are real-time sent through Ethernet to the Phantom ™ interface computer where the forces are calculated. A Phantom ™ (Sensable Co., USA) is used for 3D nano forces feeling and motion commands input, that is, the forces are felt by operator from the Phantom ™ joystick and the scanner motion command produced by joystick is sent through Ethernet into the AFM control computer to control the scanner's motion. The optical microscope and CCD camera help the operator to adjust the laser to focus on cantilever end and search for interesting area on substrate.

B Nano-imprint experiment

In this experiment, the surface of a soft material called polycarbonate is imprinted with three characters 'SIA' as shown in Fig.10., the forces during imprint is fed to Phantom^{TM} and recorded real-time. AFM nano-probe (model NSC15-F5, MickoMasch Inc., USA) with rectangle cantilevers whose force constant has been calibrated is used, and the probe is made of silicon (100) with radius of tip apex about 10nm and full tip cone angle less than 20^0.

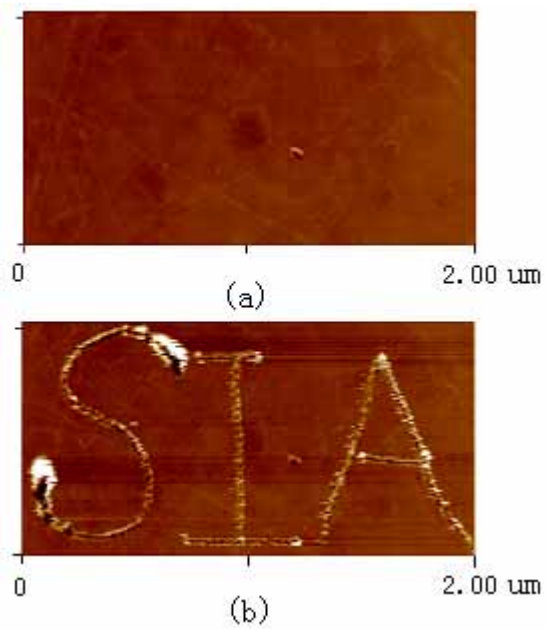

Fig.10. Nano-imprint on polycarbonate: (a) scanning image before nano-imprint; (b) scanning image after nano-imprint;

The vertical force and horizontal force along x axis during imprinting character 's' are demonstrated as shown in Fig. 11.

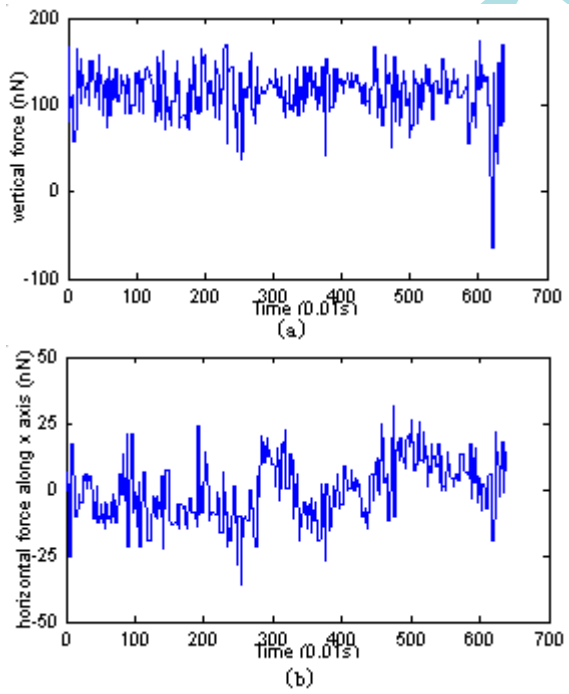

Fig. 11. Forces in nano-imprinting character 'S': (a) vertical force; (b) horizontal force along x axis

From experiments it can be seen that the nano-imprint are performed effectively and efficiently in about six seconds for imprinting character 'S', and 3D nano forces are real-time feed to Phantom^{TM}, which gives the operator real and comprehensive forces information in nano situation for helping guiding nano-imprint.

V CONCLUSION

For solving the problem of real-time feedback sensory information shortage in nanomanipulation, the micro cantilever-tip is used as a force sensor to sensing the 3D nano forces applied on AFM probe tip in nano manipulation environment. In addition, for improving the probe positioning accuracy for a sample-scanning AFM, the kinematics model of the tube scanner in the AFM is presented, and the two errors are quantitatively analyzed and corresponding methods are adopted to minimize them. As results, the operator can accurately and efficiently conduct nanomanipulation under the assistance of real-time haptic/force feedback. Nano-imprint experiments verify the effectiveness and efficiency improvement of nanomanipulation using this nanomanipulation system.

REFERENCE

[1] G. Binning, C. F. Quate, and C. Gerber. Atomic force microscope. *Physical Review Letters*, Vol. 56(9):930–933, 1986.
[2] D. M. Schaefer, R. Reifenberer, A. Patil, and R. P. Andres. Fabrication of two-dimensional arrays of nanometer-size clusters with the atomic force microscope. *Applied Physics Letters*, Vol. 66:1012–1014, February 1995.
[3] T. Junno, K. Deppert, L. Montelius, and L. Samuelson. Controlled manipulation of nanoparticles with an atomic force microscope. *Applied Physics Letters*, Vol. 66(26):3627–3629, June 1995.
[4] L. T. Hansen, A. Kuhle, A. H. Sorensen, J. Bohr, and P. E. Lindelof. A technique for positioning nanoparticles using an atomic force microscope. *Nanotechnology*, Vol. 9:337–342, 1998.
[5] A. A. G. Requicha, C. Baur, A. Bugacov, B. C. Gazen, B. Koel, A. Madhukar, T. R. Ramachandran, R. Resch, and P. Will. Nanorobotic assembly of two-dimensional structures. In *Proc. IEEE Int. Conf. Robotics and Automation*, pages 3368–3374, Leuven, Belgium, May 1998.
[6] M. Sitti and H. Hashimoto. Tele-nanorobotics using atomic force microscope. In *Proc. IEEE Int. Conf. Intelligent Robots and Systems*, pages 1739–1746, Victoria, B. C., Canada, October 1998.
[7] M. Guthold, M. R. Falvo, W. G. Matthews, S. washburn S. Paulson, and D. A. Erie. Controlled manipulation of molecular samples with the nanomanipulator. *IEEE/ASME Transactions on Mechatronics*, Vol. 5(2):189–198, June 2000.
[8] J. E. Sader, J. W. M. Chon, and P. Mulvaney, "Calibration of rectangular atomic force microscope cantilever", Review of Scientific Instruments, Vol. 70, no. 10: 403–405, 1999.
[9] R. G. Cain, M. G. Reitsma, S. Biggs, and N. W. Page, "Quantitative comparison of three calibration techniques for the lateral force microscope", Review of Scienti.c Instruments, Vol. 72, pp:3304–3312, 2001.
[10] J. Israelachvili, Intermolecular and surface forces, Academic Press London, London, UK, 1991.
[11] J. Case, L. Chilver, C. T. F. Ross. Strength of Materials and Structures (4th Edition), Elsevier, 2002.
[12] G. Binnig and D. P. E. Smith, "Single-tube three-dimensional scanner for scanning tunneling microscopy", *Review of Scientific Instruments*, vol. 57, no. 8, pp. 1688-1689,1986.
[13] Cao Wei, Honghai Zhang, Lu Tao, Wenju Li, and Hanmin Shi, "A circular arc bending model of piezoelectric tube scanners", *Review of Scientific Instruments*, vol. 67, no. 6, pp. 2286, 1996.
[14] J. A. Gallego-Juarez, "Piezoelectric ceramics and ultrasonic transducers", *Journal of Physics E: Scientific Instruments*, vol. 22, pp. 804-816, 1989.